UCRL-CONF-216863

A multi-dimensional investigation of laser conditioning in KDP and DKDP crystals

P. DeMange, R. A. Negres, C. W. Carr, H. B. Radousky, S. G. Demos

November 4, 2005

Disclaimer

A multi-dimensional investigation of laser conditioning in KDP and DKDP crystals

P. DeMange, R. A. Negres, C. W. Carr, H. B. Radousky, and S. G. Demos

Lawrence Livermore National Laboratory, 7000 East Avenue, Livermore, California 94551

ABSTRACT

We present a multi-parametric experimental investigation of laser conditioning efficiency and behavior in KDP and DKDP crystals as a function of laser wavelength, fluence, number of pulses, and conditioning protocol. Our results expose complex behaviors associated with damage initiation and conditioning at different wavelengths that provide a major step towards revealing the underlying physics. In addition, we reveal the key parameters for optimal improvement to the damage performance from laser conditioning.

1. INTRODUCTION

Laser-induced bulk damage sites arising in KDP and DKDP optics used in large-aperture laser systems is a significant deterrent to performance. The damage precursors are believed to be clusters of intrinsic defects and/or nano-particle impurities, however, identifying them has been difficult due to their size and sparse distribution. Laser conditioning is believed to be the result of the interaction of DKDP/DKDP defects (damage initiators) with sub-damage laser intensities in which the defects are annealed or modified thus providing an increase to the material damage threshold. The mechanisms leading to conditioning of these defects and the operational parameters that can optimize the effect for application on large-aperture laser systems are largely unknown. In this work, we measure the damage behaviors in pre-exposed DKDP/DKDP applying several protocols and variable excitation conditions to investigate the fundamental mechanisms of laser conditioning. The results provide important results regarding the nature of the defects responsible for damage initiation and reveal two distinct pathways leading to conditioning that depend on the pre-exposure fluence and wavelength. Moreover, these results reveal the laser parameters and protocols necessary for optimizing conditioning.

2. EXPERIMENTAL SETUP

The experimental arrangement has been described in detail elsewhere[1] but the basic setup and approach is described here briefly. The conditioning experiments are performed using a pulsed-Nd:YAG laser. The fundamental (at 1064 nm), second, and third harmonics of the output are separated using high reflectivity mirrors selective to each wavelength. The average fluence of each beam is adjusted using a waveplate and a polarizer. The three beams are then aligned to co-propagate and focused by a 200-mm focal length cylindrical lens to the bulk of the sample. The beams focus to a $1/e^2$ height of 3 mm and widths of 90 µm, 60 µm, and 40 µm for 1064, 532 and 355 nm, respectively. In order to focus each wavelength to the same location in the bulk of the crystal, we have positioned galilean telescopes in each beam line to adjust their divergence before recombination. The beam spatial profiles are measured using a 0.25 by 0.25 inch^2 CCD camera with a pixel resolution of ~ 5 µm.

The samples were cut to $1 \times 5 \times 5$ cm^3 size plates and polished on all sides. Bulk damage is produced through the focal range of the cylindrical lens, ~ 8 mm. A counter-propagating 632.8-nm beam from a HeNe laser is focused by a 250-mm focal length cylindrical lens through the back of the sample to illuminate any resulting damage pinpoints in the tested volume. Images of the damaged regions are captured orthogonally to the direction of propagation of the lasers, through the side of the sample. A × 2 magnification microscope objective followed by × 5 magnification lens is used that provides a 4.7 µm by 4.7 µm per pixel image resolution. Figure 1 shows captured images of scatter from pinpoint damage sites in bulk DKDP that demonstrate both a typical damage measurement and the manifestation of the

conditioning effect using this approach. The images capture 5.9 mm in length of the damaged volume along the direction of propagation of the beam. Figure 1a shows damage resulting from a single pulse at 15 J/cm^2 in pristine material and Fig. 1b shows damage resulting from a single pulse at 15 J/cm^2 following pre-exposure to ten pulses at 10 J/cm^2 for conditioning. The damage pinpoint density, or PPD, is measured over the volume exposed to peak laser fluence ($\pm$ 5%) which is the region enclosed by the white lines shown in each image. Comparison of the two images demonstrates that there is significantly less damage in Fig. 1b ($\sim$ 150 pp/mm^3) than in Fig. 1a ($\sim$ 1180 pp/mm^3) as a result of having pre-exposed the material to the ten pulses.
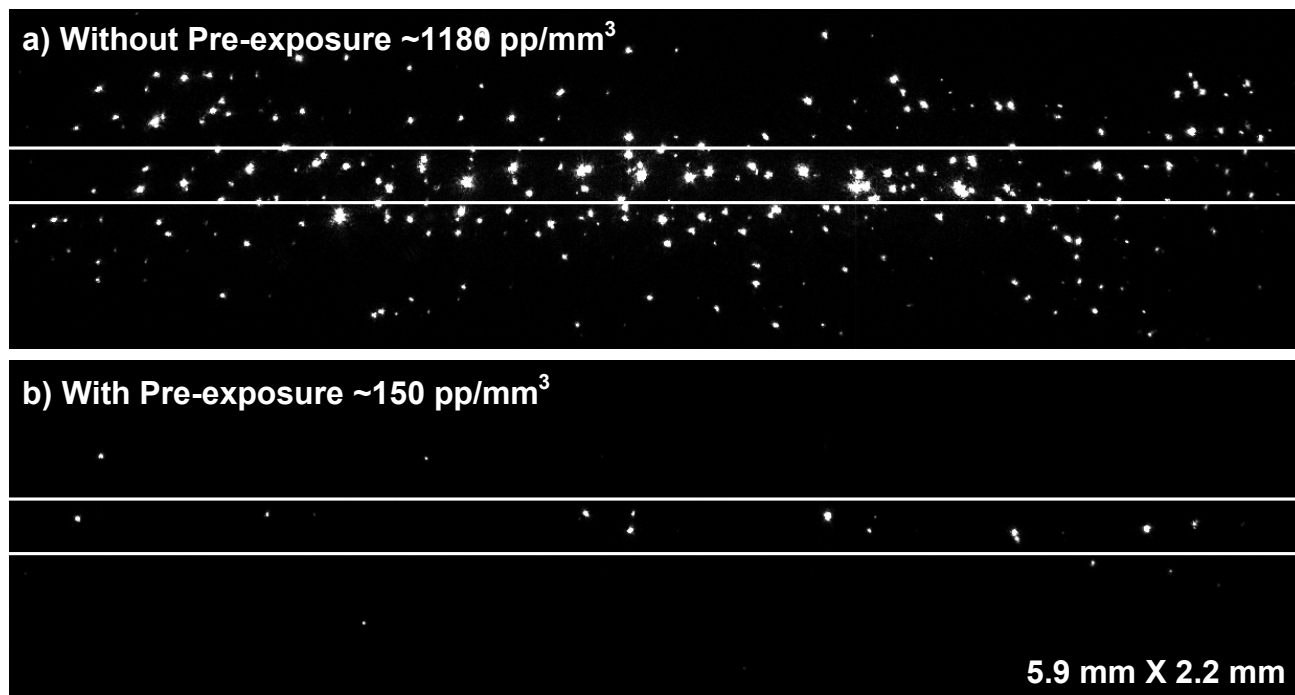

Figure 1. Scatter images of pinpoint damage sites resulting from exposure to a) one pulse at 15 J/cm^2 in pristine material ($\sim$ 1180 pp/mm^3) and b) one pulse at 15 J/cm^2 following pre-exposure to ten pulses at 10 J/cm^2 ($\sim$ 150 pp/mm^3). The PPD is measured over the volume exposed to peak laser fluence (region enclosed by the white lines).

3. EXPERIMENTS AND RESULTS

The damage performance of DKDP is investigated following pre-exposure of the material to laser pulses under variable excitation conditions including wavelength, fluence, and number of damage testing and pre-exposure pulses. We explore several conditioning protocols in order to reveal fundamental behaviors associated with the conditioning and damage initiation of the defect damage precursors as well as learn how to optimally condition the material.

3.1. Conditioning vs. Pre-exposure Fluence and Damage Testing and Pre-exposure Wavelength

The dependence of conditioning on pre-exposure fluence was measured at combinations of damage testing and pre-exposure wavelengths at 1064, 532, and 355 nm. Pristine bulk sites in conventional-growth DKDP were exposed first to ten pulses of the same fluence and then to a single higher fluence damage testing pulse. The fluence of the damage testing pulse remained the same for all sites (46 J/cm^2 for 1064 nm, 31 J/cm^2 for 532 nm, and 23 J/cm^2 for 355 nm) while the fluence of the ten pre-exposure pulses was varied. Images were recorded prior to and after irradiation at a high fluence and the PPD at peak fluence resulting from the damage testing pulse only was plotted versus the peak pre-exposure fluence.

Figures 2a-2c show the density of new damage pinpoints resulting from single-pulse damage testing at 46 J/cm^2 at 1064 nm, 31 J/cm^2 at 532 nm, and 23 J/cm^2 at 355 nm, respectively, as a function of the fluence of the ten pre-exposure pulses. There are three sets of data in each figure corresponding to pre-exposure at each of the three harmonics. It must be noted that these figures do not include the PPD resulting from pre-exposure.
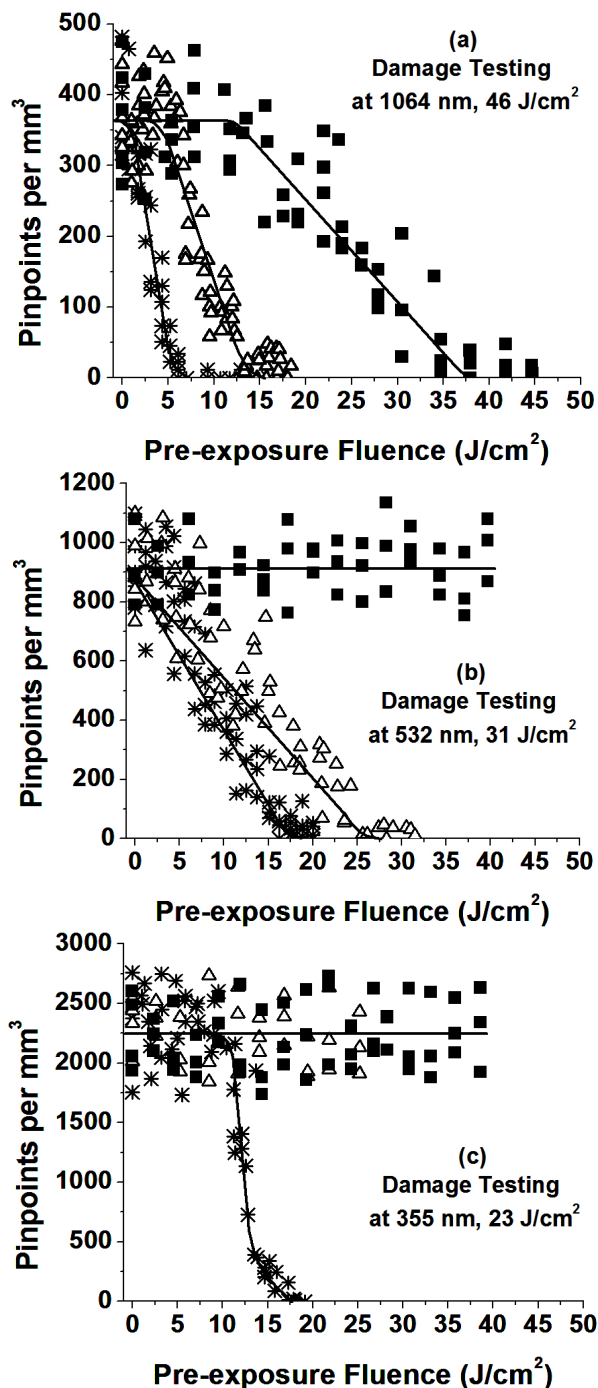

Figure 2. The density of new pinpoints resulting from damage testing pulse at a) 1064 nm at 46 J/cm^2, b) 532 nm at 31 J/cm^2, and c) 355 nm at 23 J/cm^2 as a function of the fluence of the ten pre-exposure pulses (■ = pre-exposed to 1064 nm, ◁ = pre-exposed to 532 nm, and ✳ = pre-exposed to 355 nm) in DKDP.

The density of new pinpoints resulting from damage testing at ~ 46 J/cm^2 at 1064 nm for pre-exposure at each of the three harmonics is shown in Figure 2a. Without pre-exposure, the observed PPD from damage testing is ~ 380 pp/mm^3. Following pre-exposure at 355 nm the results show that the density of new pinpoints after damage testing rapidly decreases with increase in pre-exposure fluence starting from the lowest tested pre-exposure fluence at ~ 0.7 J/cm^2. For preexposure fluence of ~ 6 J/cm^2, the density of new pinpoints decreases to almost ~ 0 pp/mm^3 (from the original ~ 380 pp/mm^3) while the pre-exposure is still below the damage threshold of the material (located at ~ 8 J/cm^2). Pre-exposure at 532 nm shows no conditioning until ~ 6 J/cm^2, demonstrating the presence of a threshold fluence for conditioning. A linear decrease in the density of new pinpoints in then observed with further increase in pre-exposure fluence. Damage testing results in very little or no additional damage for pre-exposure of ~ 14 J/cm^2 and above but this pre-exposure fluence is above the damage threshold of the material (located at ~12 J/cm^2). Pre-exposure at 1064 nm also shows that a threshold pre-exposure fluence exists for conditioning located at ~ 13 J/cm^2 followed by a linear decrease in the PPD. The density of new pinpoints decreases to ~ 0 pp/mm^3 with pre-exposure at ~ 40 J/cm^2, well above the damage threshold at 1064 nm which is at ~24 J/cm^2.

Figure 2b shows the three sets of data for damage testing at ~ 31 J/cm^2 at 532 nm in material pre-exposed at each of the three harmonics. Damage testing without pre-exposure provides ~ 900 pp/mm^3. With pre-exposure at 355 nm, the density of new pinpoints from damage testing appears to decrease linearly with increase in pre-exposure fluence starting from the lowest tested pre-exposure fluence. For pre-exposure above ~ 18 J/cm^2, almost no new pinpoints are observed from damage testing. Similarly, pre-exposure at 532 nm results in a linear decrease in the density of new pinpoints, however, the best conditioning occurs at a much higher pre-exposure fluence of ~ 32 J/cm^2. Damage testing following pre-exposure at 1064 nm up to ~ 40 J/cm^2 indicates no improvement to the damage performance.

Figure 2c shows the three data sets corresponding to the damage testing at ~ 23 J/cm^2 at 355 nm and pre-exposure at each harmonic. Damage testing without pre-exposure provides ~ 2250 pp/mm^3. Similar to the behavior observed for damage testing at 1064 nm and pre-exposure at both 1064 and 532 nm (shown in Fig. 2a), pre-exposure at 355 nm demonstrates the presence of a threshold fluence for conditioning at ~ 10 J/cm^2. However, the density of new pinpoints then rapidly decreases with increasing fluence. Pre-exposure at 532 and 1064 nm up to fluences of ~ 25 J/cm^2 and ~ 38 J/cm^2, respectively, indicate no improvement to the damage performance.

The results show three different characteristic behaviors. For damage testing at 1064 nm, a "threshold" fluence for conditioning is observed followed by a linear decrease in damage density at higher pre-exposure fluence. For damage testing at 532 nm, a linear behavior is observed with no noticeable threshold fluence. For damage testing at 355 nm, a sharp nonlinear or "step-threshold" behavior is the dominant feature. Elsewhere in this proceedings experimental results have indicated that the defects responsible for damage initiation at 532 and 355 nm are the same and the defects responsible for damage initiation at 1064 nm are different (to those at 532 and 355 nm).[2,3] These different behaviors, if arising from the same type of defects responsible for damage initiation, suggest the presence of multiple pathways leading to conditioning.

3.2. Conditioning vs. Damage Testing and Pre-exposure Fluence

In order to learn the extent of laser conditioning in improving damage performance of these materials one needs to also consider the dependence of the conditioning threshold of individual defects on their damage initiation threshold. More specifically, is there a specific conditioning threshold for all 355-nm damage initiating defects or is this threshold different for each initiator? If the latter is true, then does the conditioning threshold of each initiator relate to the individual damage initiation threshold which may tie both processes to a characteristic property of the initiators (e.g. size or density)? These questions may be hard to address but some insight can be offered by studying the damage behavior at different laser fluences using the same conditioning protocol used above. Specifically, experiments were performed to investigate the conditioning effectiveness versus pre-exposure fluence for two damage testing fluences with both pre-exposure and damage testing at 355 nm. In one case the damage testing fluence was 15-16 J/cm^2 while in the other case the damage testing fluence was 20-21 J/cm^2. In both cases sites were exposed to a single damage testing pulse following exposure to ten pulses of the same (pre-exposure) fluence.

Figure 3 shows the density of new pinpoints resulting from damage testing as a function of the pre-exposure fluence, for both experiments. The results of damage testing at 20-21 J/cm^2 at 355 nm are shown as solid circles and the results of damage testing at 15-16 J/cm^2 at 355 nm are shown as open circles. The results show that the conditioning threshold in

both experiments starts at ~ 6.5 J/cm^2. A drop of ~ 1000 pinpoints per mm^3 for damage testing at both 15-16 J/cm^2 and 20-21 J/cm^2 occurs at pre-exposure fluences between ~ 6.5 J/cm^2 and ~ 10 J/cm^2 (depicted in Fig. 3). This demonstrates that the population of conditioned defects for this pre-exposure, equivalent to ~ 1000 pinpoints per mm^3, is independent of the damage testing fluence. Moreover, this pre-exposure only conditions a subset of the defect population. The population of damage initiators that initiates damage at 15-16 J/cm^2 has been mostly diminished (some initiators erupt to form damage sites during pre-exposure). One then may argue that the defects that initiate damage at 15-16 J/cm^2 can be conditioned with pre-exposure fluences at 10 J/cm^2. The PPD profile obtained with damage testing at 20-21 J/cm^2 shows that further pre-exposure up to 17 J/cm^2 reduces the PPD by another ~ 1300 pinpoints per mm^3 indicating that an additional population of defects condition at a higher fluence. This result indicates that pre-exposure at a fixed fluence at 355 nm conditions only a portion of the whole population of defects leading to damage initiation at 355 nm and has no effect on the remaining defects.
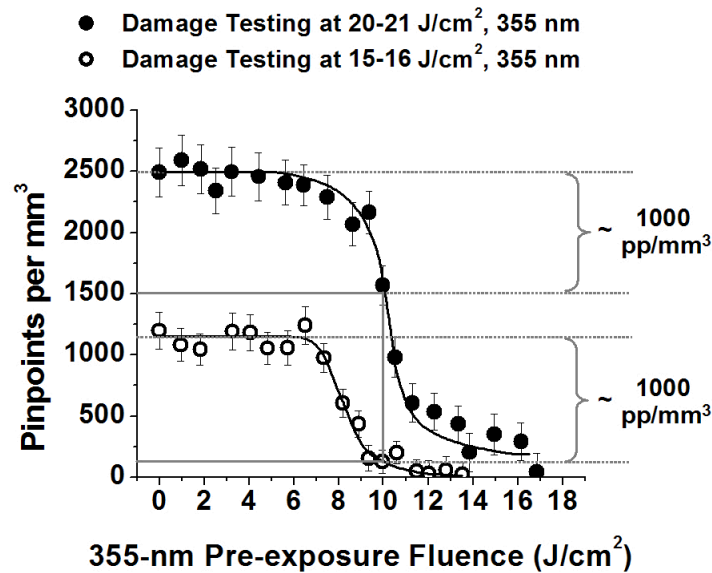

Figure 3. The total PPD resulting from both damage testing and pre-exposure to ten pulses at 355 nm as a function of the pre-exposure fluence. O = damage testing at 15-16 J/cm^2 and ● = damage testing at 20-21 J/cm^2.

3.3. Conditioning vs. Pre-exposure Number of Pulses and Total Energy Using Ramping Method

The damage performance at 355 nm of material conditioned at 355 nm using the ramped-fluence pre-exposure method was explored, looking specifically at the dependence of conditioning on the fluence step size and number of pre-exposure pulses per step in the ramping protocol. This experiment provides information on the optimal ramping fluence protocol using the smallest level of exposure (i.e., the largest fluence step sizes and the least number of pulses per step) as well as the dependence of conditioning of the defects responsible for damage on the total pre-exposure energy and intensity. Pristine bulk sites were exposed to gradually increasing (i.e., ramped) peak laser fluences in 1- or 2-J/cm^2 steps starting at 1 J/cm^2. At each fluence step, the material was exposed to a fixed number of pulses (1, 2, 5 or 10 pulses). The fluence was ramped up to the highest fluence at which no damage would be observed using the CCD camera. Sites within the ramp-pre-exposed volume were then exposed to single damage testing pulses at various fluences and the PPD was measured.

Figure 5 shows the PPD resulting from damage testing as a function of the testing fluence for several ramped pre-exposure protocols. The ramping pre-exposure protocol corresponding to each damage density profile is simplified using the following functional description: P(ramping fluence step in J/cm^2, # of pulses at each step, maximum fluence reached during ramping without damaging). The results show that the onset of damage in the pristine material is ~ 5 J/cm^2. A

significant increase to the fluence onset of damage (to ~ 7 J/cm^2 from ~ 5 J/cm^2 in the pristine material) and the overall damage performance is observed with ramping pre-exposure using as large of a fluence step as 2 J/cm^2 and as little as 1 pulse per step, demonstrated by the P(2,1,5) damage profile. The P(2,2,5) profile shows that the increase in number of pulses from 1 to 2 per fluence step provides no increase to neither the maximum fluence reached during pre-exposure nor the level of conditioning. The P(1,1,7) and P(2,10,7) damage profiles are similar, both showing a significant increase to the fluence onset of damage to ~ 9 J/cm^2 and overall damage performance. Their comparison suggests that the smaller step size of the P(1,1,7) profile compensates for the greater number of pulses in the P(2,10,7), although both reach the same maximum fluence of 7 J/cm^2 during ramping pre-exposure. The P(1,2,8) profile shows that the increase in number of pulses per step to 2 from 1 in the P(1,1,7) profile results both in a higher maximum ramping pre-exposure fluence and better conditioning (a fluence onset of damage of ~ 10 J/cm^2 compared to ~ 9 J/cm^2). The P(1,10,9) profile reaches the highest maximum ramping pre-exposure fluence and shows an increase to the fluence onset of damage to ~ 11 J/cm^2. An additional 1000 pulses at 9 J/cm^2 on top of the P(1,10,9) ramping protocol shows very little improvement to the overall damage performance and only ~ 1 J/cm^2 increase to the fluence onset of damage from the P(1,10,9) only ramping protocol.

The results show that conditioning becomes increasingly better with smaller ramping fluence steps and greater numbers of pulses. However, we observe a direct correlation between the relative level of conditioning and the maximum fluence reached during ramping pre-exposure without damaging the material. Moreover, the maximum fluence becomes higher with smaller ramping fluence steps and greater numbers of pulses. With the addition of 1000 pulses to the P(1,10,9) protocol at the maximum ramping pre-exposure fluence of 9 J/cm^2 there is very little additional improvement to the overall damage performance compared to the P(1,10,9) protocol only. This demonstrates that the fluence step size or number of pulses per step individually is not the important factor but that the maximum ramping pre-exposure reached is the critical parameter in providing the best level of conditioning. In this material, an approximately 2% increase to the damage performance can be achieved with ramping pre-exposure with fluence steps as large as 1 J/cm^2 and as few pulses as 10 per fluence step.
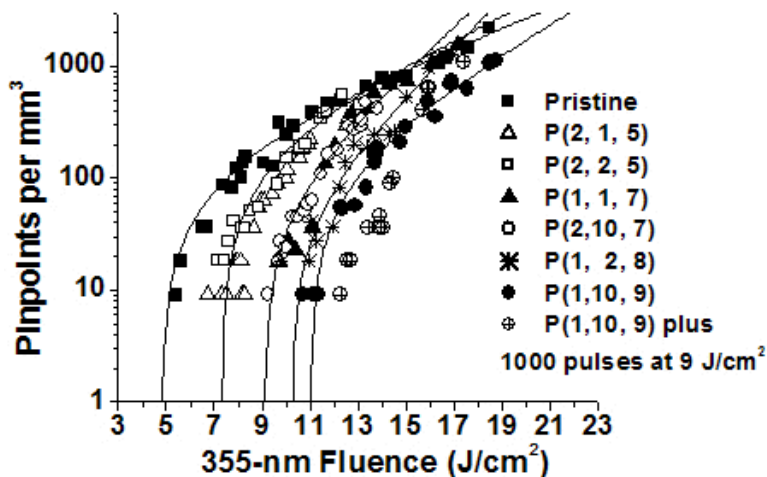

Figure 5: Damage density profiles at 355 nm in DKDP on a log–linear scale without and with conditioning using various fluence ramping protocols. The function that corresponds to each damage density profile describes the ramping protocol as follows: P(ramping fluence step in J/cm^2, # of pulses at each step, maximum fluence reached during ramping without damaging). The lines shown are the best fits to each data set.

3.3. Conditioning vs. Testing and Pre-exposure Wavelength Using Ramping Method

Ramped-fluence pre-exposure was used as a method to explore optimal improvement to the damage performance at all of the nine combinations of damage testing and pre-exposure at 1064, 532, and 355 nm. In addition to learning the level of conditioning that may be achieved and the necessary pre-exposure wavelengths for providing this optimal conditioning for operation at a specific wavelength, we also gain insight into the wavelength absorption characteristics

leading to conditioning of the defects responsible for damage. The best performing pre-exposure fluence ramping protocol from the above results was used (i.e., P(1,10,X) protocol or exposing pristine bulk volumes to gradually increasing fluence levels in 1 J/cm^2 steps starting at 1 J/cm^2). The volumes were rastered by setting the sample stage speed such that each volume was exposed to 10 pulses at peak fluence at each fluence step. The fluence was ramped up to the highest fluence at which no damage was observed by the CCD camera. This highest conditioning fluence was approximately 11 J/cm^2 at 355 nm, 17 J/cm^2 at 532 nm, and 24 J/cm^2 at 1064 nm. The conditioned volume was then tested with single damage testing pulses with the fluence varying at each new site. An image of the damage was then captured for measurement of the resulting PPD.

Figure 4 shows data profiles of the PPD as a function of fluence, for damage testing at 1064, 532 and 355 nm. These profiles demonstrate the damage behavior of a DKDP sample both without and with conditioning at each harmonic using the fluence-ramping method. The plots are on a semi-log scale and data fit lines are drawn in as a guide to the eye. The PPD profiles obtained under 1064-nm damage testing are shown in Fig. 1a. The observed onset of damage of the unconditioned material is found to be ~ 20 J/cm^2. Pre-exposure at 1064 nm demonstrates a substantial increase in the onset of damage to 30 J/cm^2. Pre-exposure at 532 nm increases the onset of damage even more to ~37.5 J/cm^2, and 355-nm pre-exposure shows at least 2× increase. The PPD profiles obtained under 532-nm damage testing are shown in Fig. 1b. The onset of damage of the unconditioned material is found to be ~ 10 J/cm^2. An increase in the onset of damage to 15 J/cm^2 is achieved by pre-exposure at 355 nm while pre-exposure at 532 nm shows a larger increase in the onset of damage to nearly 19 J/cm^2. The PPD profiles obtained under 355-nm damage testing are shown in Fig. 1c. These results show that pre-exposure at 355 nm increased the onset of damage to above 12.5 J/cm^2 from the ~ 8 J/cm^2 measured in the unconditioned material. However, pre-exposure at 1064 nm and 532 nm results in no noticeable increase in the 355-nm onset of damage.
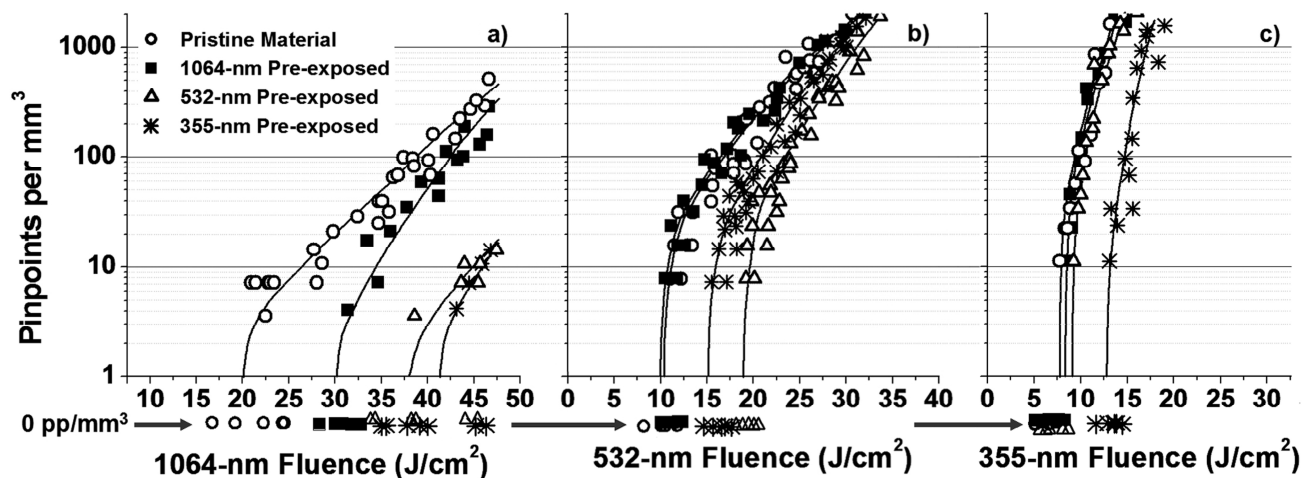

Figure 4. PPD profiles for a DKDP crystal sample on a semi-log scale at a) 1064, b) 532, and c) 355 nm. The testing fluences for which no damage was observed (i.e., 0 pp/mm^3) are indicated by the arrow. The curves are a guide to the eye.

As a general rule, conditioning occurs for pre-exposure at wavelengths equal to or shorter than that used for damage testing. Figure 4b shows that pre-exposure to 532-nm pulses provides better conditioning for 532-nm operation than pre-exposure to 355-nm pulses, an opposite trend to that observed in Fig. 4a, where the lower wavelengths provided better conditioning for 1064-nm testing. This is likely due to the ability to reach higher fluence during pre-exposure at 532 nm. Damage testing at 355 nm indicated that pre-exposure at either 1064 nm or 532 nm provides no improvement to damage resistance while, in contrast, pre-exposure at 355 nm shows significant improvement.

3.5. Conditioning shelf lifetime

Understanding the effectiveness of conditioning over time is a concern with regard to its application to KDP/DKDP optics in large-aperture laser systems. We performed an experiment to assess the damage performance of bulk DKDP without and with conditioning over a period of ~ 6 months. The conditioning was performed with both 3-ns and 800-ps flat-top 355-nm pulses on LLNL's OSL facility. These pulse-lengths were used in order to gather data at two points within the pulse-length region determined to provide significant conditioning.[4] The laser beam was ~ 1 cm in diameter and two separate regions of the sample were exposed to ramping fluence at each pulse-length. The damage testing was performed with 3-ns pulses using the system described in this work. Damage density profiles of the pristine material and both conditioned regions were measured 4 days, 34 days, and 191 days after conditioning.

Figure 6 shows the PPD resulting from single 3-ns damage testing pulses at various fluences in the pristine, 3-ns ramp-conditioned, and 800-ps ramp-conditioned DKDP. The damage profiles of the pristine material are indicated by squares, the 3-ns conditioned material by circles, and the 800-ps material by triangles. The filled shapes indicate testing 4 days after conditioning, the unfilled shapes after 34 days, and the shapes with an "X" after 191 days. The onset of damage of the pristine material takes place at ~ 5 J/cm^2. Four days after conditioning, the onset of damage occurs at fluences of ~ 7 J/cm^2 and ~ 9 J/cm^2 for the 3-ns and 800-ps conditioned regions, respectively. The damage performance of the 3-ns and 800-ps conditioned materials begin to converge with that of the pristine material at higher PPDs. Specifically, the PPD profile of the 3-ns conditioned material overlaps with that of the pristine material for PPDs of ~1000 pp/mm^3 and higher. In this PPD range, the PPD profile of the 800-ps conditioned material is still below that of the pristine material with the profiles appearing to convergence at higher PPDs. The damage profiles of the material after 34 and 191 days indicate no change to the damage performance of either conditioned regions.
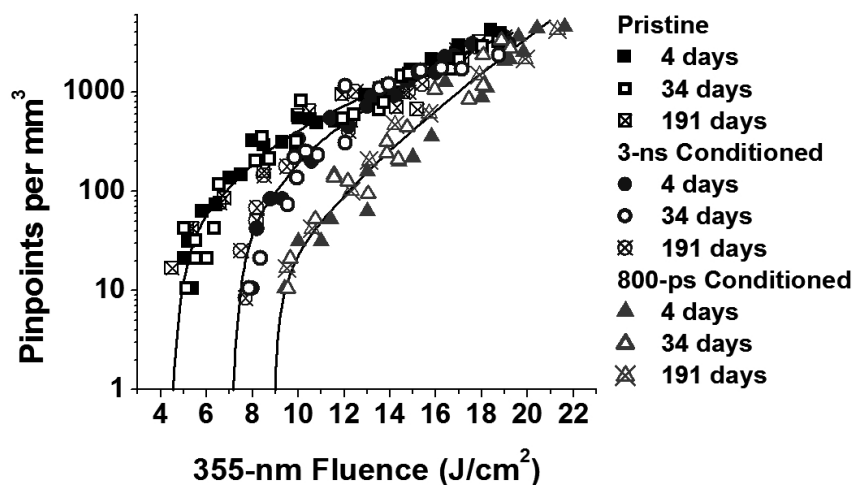

Figure 6. Damage density profiles on log-linear scale in a DKDP sample without conditioning (shown as squares), with conditioning at 3 ns (shown as circles), and 800 ps (shown as triangles) measured after 4 days (solid shapes), 34 days (unfilled shapes), and 191 days (shapes with an "X"). The three curves are fits to the three profiles measured after 4 days, to guide the eye.

4. CONCLUSION

The ramp conditioning results show that the level of conditioning achieved at 355 nm depends on the maximum fluence that can be reached during conditioning without causing damage. This maximum fluence depends on the ramping fluence step size and number of conditioning pulses. Furthermore, conditioning is demonstrated to take place using wavelengths at or below the testing wavelength. The results of investigating conditioning as a function of the pre-exposure fluence reveal that a "threshold" pre-exposure fluence is necessary when conditioning for 355-nm operation while, on the other hand, a linear dependence of conditioning on pre-exposure fluence is observed when conditioning for 532-nm operation. These different behaviors arising from conditioning of the same set of initiators suggest that there may be more than one conditioning pathway in KDP crystals that depend on the laser intensity and wavelength of the

conditioning pulses. Damage testing and conditioning at different fluences at 355 nm suggests that pre-exposure at a fixed fluence conditions only a subset of the defect population, instead of improving the damage behavior of the entire population of damage initiating defects.

ACKNOWLEDGEMENTS

REFERENCES

1. P. DeMange, C. W. Carr, H. B. Radousky, and S. G. Demos, "System for evaluation of laser-induced damage performance of optical materials for large aperture lasers," *Rev. Sci. Instrum*. **75**, 3298 (2004).
2. R. A. Negres, P. DeMange, H. B. Radousky, S. G. Demos, "Laser-Induced Damage in DKDP Crystals under Simultaneous Exposure to Laser Harmonics," in these proceedings **5991-30**.
3. P. DeMange, R. A. Negres, H. B. Radousky, S. G. Demos, "Different precursor populations revealed by microscopic studies of bulk damage in KDP and DKDP crystals," in these proceedings **5991-87**.
4. J. J. Adams, T. L. Weiland, J. R. Stanley, W. D. Sell, R. L. Luthi, J. L. Vickers, C. W. Carr, M. D. Feit, A. M. Rubenchik, M. L. Spaeth, and R. P. Hackel, "Pulse-length dependence of laser conditioning and bulk damage in KD_2PO_4," in *Laser-Induced Damage in Optical Materials: 2004*, Gregory J. Exarhos, Arthur H. Guenther, Norbert Kaiser, Keith L. Lewis, M. J. Soileau, Christopher J. Stolz, Eds., *Proc. SPIE* **5647**, 265-278, 2005.